PHYSICAL REVIEW C **92**, 065502 (2015)

# Measurement of the branching ratio for the $\beta$ decay of $^{14}$O

P. A. Voytas* and E. A. George
*Physics Department, Wittenberg University, Springfield, Ohio 45501, USA*

G. W. Severin,† L. Zhan,‡ and L. D. Knutson
*Physics Department, University of Wisconsin-Madison, Madison, Wisconsin 53706, USA*

(Received 11 August 2015; published 30 December 2015)

We present a new measurement of the branching ratio for the decay of $^{14}$O to the ground state of $^{14}$N. The experimental result, $\lambda_0/\lambda_{\text{total}} = (4.934 \pm 0.040\,(\text{stat.}) \pm 0.061\,(\text{syst.})) \times 10^{-3}$, is significantly smaller than previous determinations of this quantity. The new measurement allows an improved determination of the partial half-life for the superallowed $0^+ \to 0^+$ Fermi decay to the $^{14}$N first excited state, which impacts the determination of the $V_{ud}$ element of the CKM matrix. With the new measurement in place, the corrected $^{14}$O $\mathcal{F}t$ value is in good agreement with the average $\mathcal{F}t$ for other superallowed $0^+ \to 0^+$ Fermi decays.

DOI: 10.1103/PhysRevC.92.065502 PACS number(s): 23.40.Bw, 24.80.+y, 27.20.+n

## I. INTRODUCTION

The Cabibbo-Kobayashi-Maskawa (CKM) matrix parametrizes the extent to which quark energy eigenstates are mixed in charge-changing weak decay processes. For example, the weak interaction couples the $u$ quark to a mixture of $d$, $s$, and $b$ quarks, and the "weak interaction eigenstate" can be written in the form,

$$|d'\rangle = V_{ud}|d\rangle + V_{us}|s\rangle + V_{ub}|b\rangle, \tag{1}$$

where $|d\rangle$, $|s\rangle$, and $|b\rangle$ are the quark mass eigenstates, and where $V_{ud}$, $V_{us}$, and $V_{ub}$ are elements of the CKM matrix.

Nuclear $\beta$ decay involves weak transitions between $u$ and $d$ quarks, and one consequence is that decay rates are proportional to $|V_{ud}|^2$. In fact, the value of $V_{ud}$ is most accurately determined from an analysis of measured rates for superallowed Fermi decays, i.e., for $0^+ \to 0^+$ transitions between nuclear isobaric analog states. In a recent comprehensive analysis of the world data on decays of this kind, Hardy and Towner (HT) [1] report the result $V_{ud} = 0.97417 \pm 0.00021$.

One of the important isotopes in the analysis of Ref. [1] is $^{14}$O. The nucleus $^{14}$O has a $0^+$ ground state and a half-life of 70.62 s [2], and decays by positron emission. More than 99% of the decays proceed by the superallowed Fermi transition to the 2.313 MeV $0^+$ first excited state of $^{14}$N, while most of the remaining decays populate the $^{14}$N ground state. The lifetime of $^{14}$O is well known [2], but determination of the $ft$ value for the $0^+ \to 0^+$ transition requires knowledge of the ground-state branching ratio, $R$.

We are aware of three previous measurements of this quantity. Sherr *et al.* [3] report the value $R = (0.6 \pm 0.1)\%$, while Frick *et al.* [4] find $R = (0.65 \pm 0.05)\%$. Most recently, in 1966, Sidhu and Gerhart [5] obtained the result $R = (0.61 \pm 0.01)\%$.

All three measurements have been discussed and reanalyzed by Towner and Hardy [6], and based on that reanalysis HT have adopted the value $R = (0.571 \pm 0.068)\%$ for use in the analysis of the superallowed $0^+ \to 0^+$ transitions. We will comment further on the previous determinations of $R$ in Sec. IV.

In this paper we shall present a new measurement of the branching ratio $R$. When combined with the recent precise determination of the $^{14}$O $Q$ value [7], the new measurement leads to a significant reduction in the uncertainty of the $^{14}$O $\mathcal{F}t$ value.

## II. DESCRIPTION OF THE EXPERIMENT

The measurements were carried out at the University of Wisconsin Nuclear Physics Laboratory. Many of the experimental details, including a description of the apparatus, are given in a previous publication [8], denoted in the following as GVSK. Briefly, radioactive $^{14}$O is produced by bombarding a nitrogen gas target with protons of about 8 MeV. $^{14}$O produced in the target cell is incorporated into water, separated cryogenically from the nitrogen gas, and delivered to a beta spectrometer. There the sample is deposited onto a cold, 13-$\mu$m-thick aluminum backing foil and inserted into the spectrometer for counting.

The spectrometer [9] was constructed following the basic design principles of a "Wu Spectrometer" [10] with fields provided by superconducting magnets. Positrons that pass through the spectrometer are detected in a nominally 5-mm-thick lithium-drifted silicon [Si(Li)] detector. The acceptance function of the spectrometer has a full width half maximum (FWHM) of about 2% and a peak solid angle of roughly 0.5 sr. The centroid of the acceptance function occurs at a momentum of approximately 248 keV/c per A of current, and the calibration is known to an accuracy of better than 1 part in $10^4$ [9].

Measurements of the beta spectra for the ground- and excited-state transitions were obtained with different

*pvoytas@wittenberg.edu
†Present address: The Hevesy Laboratory, Center for Nuclear Technologies, Technical University of Denmark, Frederiksborgvej 399, 4000 Roskilde, Denmark.
‡Present address: Facebook Inc., 1 Hacker Way, Menlo Park, CA 94025.

 

experimental procedures. The need for separate procedures is brought on by the presence of low energy positrons from decay of $^{15}$O, produced by $^{15}$N($p$,$n$), and from $^{11}$C, produced by $^{14}$N($p$,$\alpha$). For the ground-state measurements the counting rates are low, but the positron energies are high and effects from the contaminant positrons are, for the most part, irrelevant. On the other hand, the excited-state measurements benefit from much higher rates, but counts from the contaminants need to be eliminated.

### A. Ground-state measurements

Most of the relevant experimental details concerning the ground-state measurements are given in GVSK. In that publication we reported measurements of the shape of the ground-state $\beta$ spectrum for positron kinetic energies ranging from 1.9 to 4.0 MeV. The lowest energy is 90 keV above the endpoint of the excited-state decay, while the highest is close to the ground-state endpoint energy, 4.12 MeV.

In the GVSK experiment, the spectrum shape was determined by preparing an $^{14}$O source and recording the number of detected positrons at several spectrometer currents in sequence. The process of source preparation followed by measurements at several currents, referred to as a cycle, was repeated many times to achieve the desired statistical accuracy. The measurements presented in GVSK determine ratios of the ground-state beta spectrum intensity at different currents, but do not fix the absolute normalization.

To obtain the branching ratio, we need to make a connection between measurements taken above and below the endpoint of the excited-state transition. The connection is made by using measurements at a spectrometer current of 8.8 A as a point of contact. At 8.8 A, the centroid of the acceptance function corresponds to a positron kinetic energy of 1.731 MeV. This energy is a bit below the 1.809 MeV excited-state endpoint, but still high enough so that the results are not affected by positrons from $^{15}$O or $^{11}$C.

To supplement the data presented in GVSK, we collected measurements for cycles in which the spectrometer current was moved between 8.8 and 11.0 A, the latter being well above the excited-state endpoint. Typically, a source would be counted for 15 s at 8.8 A and then for 53 s at 11.0 A. For the next source we would count for 60 s at 11.0 A and then 30 s at 8.8 A. The process was repeated for many such cycles.

Accumulated Si(Li) energy spectra for a typical run of this kind are shown in Fig. 1. At each current there is a primary peak corresponding to events in which the positron deposits its full energy in the detector. Counts above the main peak occur from processes in which the positron energy pulse is supplemented with energy deposited by one or both of the 511-keV annihilation $\gamma$ rays, while counts below the primary peak but above channel 120 arise mainly from events in which the positron backscatters out of the Si(Li) detector, depositing only a portion of its kinetic energy.

Backgrounds from decay of $^{11}$C which has migrated to positions close to the detector (see GVSK) and from 511-keV $\gamma$ rays originating from inside the spectrometer are responsible for the increased count rate below about channel 120.

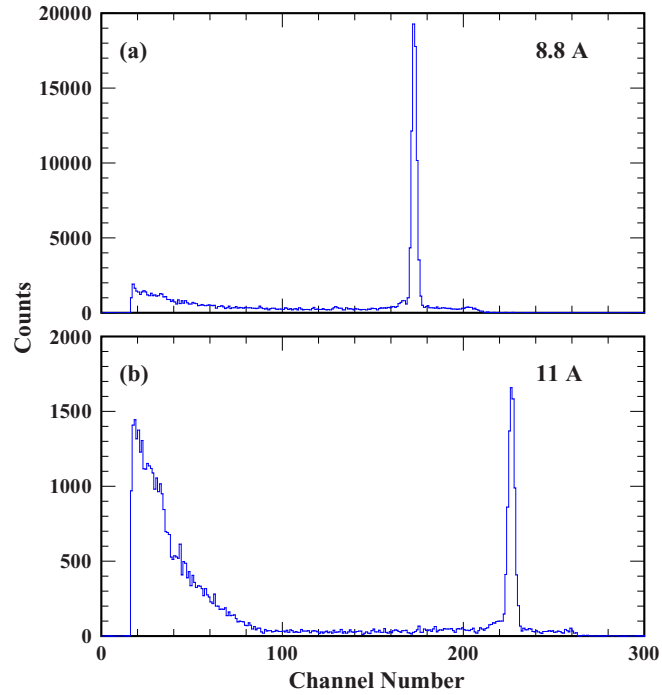


FIG. 1. (Color online) Si(Li) spectra obtained with the spectrometer current set at 8.8 and 11.0 A. These settings are, respectively, just below and well above the endpoint of the excited-state transition. The measured counts have been rescaled so that the two spectra correspond to the same number of $^{14}$O decays. Note the factor of 10 difference in scales for the two spectra.

The measurements were analyzed following the procedures outlined in GVSK. First, the raw counting rates are corrected for backgrounds. We include room backgrounds, backgrounds associated with the proton beam, and backgrounds arising from 2.3-MeV $\gamma$ rays emitted following decay of $^{14}$O to the first excited state of $^{14}$N. We also correct for "bad events," which occur when positrons reach the Si(Li) detector after scattering from slit edges, the aluminum backing foil, or other objects within the spectrometer. The room and beam backgrounds are measured, while Monte Carlo simulations are used to estimate the backgrounds from bad events and 2.3-MeV $\gamma$ rays.

Let $S_R$ represent the measured number of counts within some energy window for a given run and a given current. If $B$ is the associated background, then the corrected event sum $N_R(I)$ is given by

$$N_R(I) = (S_R - B)F_S/F_D. \quad (2)$$

Here $F_D$ is a decay factor defined as the fraction of all $^{14}$O decays that occur while counting at a specific current, while $F_S$ corrects for good positron events that lie outside of the summation window. We determined this latter quantity by using clean positron spectra from $^{66}$Ga decay in combination with Monte Carlo simulations (see GVSK). Basically, Eq. (2) corrects for backgrounds and subthreshold events, and extrapolates the measured sums back to a common start time.

The quantities $N_R$ for a given run depend on the source activity for that run and also on a quantity $\bar{n}(I)$, defined to be the beta spectrum intensity, $n(p) \equiv \frac{dn}{dp}$, integrated over the

acceptance of the spectrometer.[1] The activity factor cancels if we take ratios of the corrected event sums, and consequently we are able to determine the quantity $\bar{n}(8.8\ \mathrm{A})/\bar{n}(11.0\ \mathrm{A})$. The best-fit value of this ratio is found to be $8.480 \pm 0.048$.

From this measurement we can determine the ratio of the spectrum intensities $n(p)$ at the two currents. The acceptance width of the spectrometer scales with the momentum, and consequently $n(p)$ is obtained by taking $\bar{n}(I)/p$ and applying a small correction for the curvature of the $\beta$ spectrum. The result is

$$\frac{n(8.8\ \mathrm{A})}{n(11.0\ \mathrm{A})} = \frac{n(2.183\ \mathrm{MeV/c})}{n(2.729\ \mathrm{MeV/c})} = 10.39 \pm 0.06, \qquad (3)$$

where the quoted uncertainty includes statistics only. With this result we can normalize the $\beta$ spectrum of GVSK to the value at 8.8 A.

In GVSK we assumed that the ground-state $\beta$-spectrum intensity is of the form,

$$n_0(p) = p^2\,(E - E_0)^2\,F(p,Z)\,C(E), \qquad (4)$$

where $p$ $(E)$ is the positron momentum (energy), $E_0$ is the endpoint energy, $F(p,Z)$ is a Fermi function, and $C(E)$ is a shape factor. Our Fermi function is

$$F(p,Z) = F_0(p,Z)\,L_0^A\,C_A\,R_A\,Q\,g(E,E_0), \qquad (5)$$

where $F_0$ is the usual Fermi function for a point charge nucleus with lepton wave functions evaluated at the nuclear surface (see, for example, Ref. [11]), $g(E,E_0)$ is a radiative correction factor calculated following Sirlin [12], $L_0^A$ and $C_A$ are finite size corrections as given by Wilkinson [11], and $R_A$ and $Q$ are corrections for recoil and screening, respectively, again calculated according to Wilkinson [13]. Finally the shape factor is of the form,

$$C(E) = k[1 + a'W + b'/W + c'(W - W_c)^2], \qquad (6)$$

where $W$ is the positron total energy in units of its rest energy, $a'$, $b'$, and $c'$ are constants, and $W_c$ is the $W$ value corresponding to a positron kinetic energy of 2.75 MeV. In GVSK, the shape parameters $a'$ and $c'$ are determined by fitting measurements, while $b'$, which is relatively unimportant, is fixed at its theoretical value.

The resulting ground-state $\beta$ spectrum is shown by the solid curve in Fig. 2. The curve is plotted on a scale set by the condition $n(p) = 1$ at 8.8 A. This is accomplished by using the $8.8\ \mathrm{A} \leftrightarrow 11.0$ A measurements, as summarized in Eq. (3), to determine the constant $k$ in Eq. (6). Effectively, what this does is to fix the $n(p)$ curve at $p = 2.729$ MeV/c to the value 0.0962. Ultimately, we will use this calculated curve to determine the branching ratio, and consequently it is important to know that the spectrum shape is well determined.

The data points in Fig. 2 represent a sample of the measurements that were used in GVSK to determine the $\beta$-spectrum shape, and are included to illustrate the quality of the data set. To generate the points we collect data from

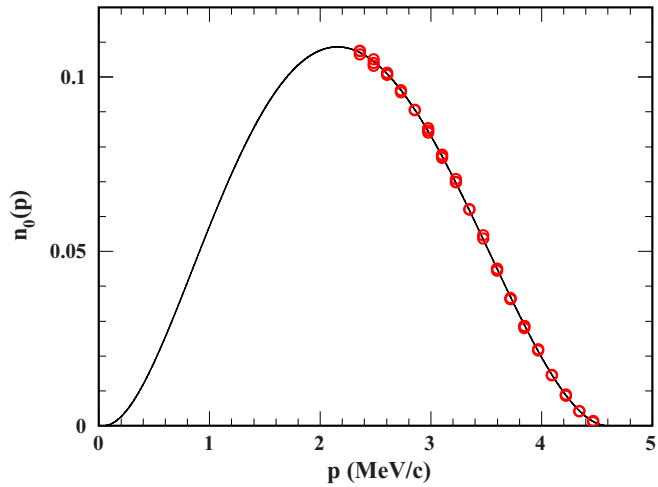


FIG. 2. (Color online) Measurements of the $^{14}$O $\beta$-spectrum intensity for momentum values above the endpoint of the excited-state transition. The curve is from GVSK, with normalization fixed by the measurements reported here. The open circles represent a sample of the data used in GVSK to fix the shape of the $\beta$ spectrum. Either two or three points are plotted at each momentum value, because the partial data sets have many overlap points. The error bars, which are not plotted, are smaller than the symbols.

all runs in which measurements were taken at a particular sequence of currents, for example, 10.0, 12.0, 14.0, and 16.0 A. Following procedures outlined in GVSK, we fit this subset of measurements with a theoretical curve of the form Eq. (4) treating $a'$ and $c'$ of Eq. (6) as free parameters. Each curve is then normalized to $n(2.729\ \mathrm{MeV/c}) = 0.0962$, which fixes $k$, and the data (which lack an absolute normalization) are rescaled to the newly determined curve. This analysis was carried through for 10 independent subsets of the data. The subsets chosen were the ones that determined the shape parameters with greatest statistical precision. All of the resulting points are shown in the plot.

### B. Excited-state measurements

We must now obtain analogous results for decay to the first excited state of $^{14}$N. As noted earlier, the main complication in this case is the presence of positrons from decay of $^{11}$C and $^{15}$O. We separate out the contribution from $^{14}$O by exploiting the fact that the three isotopes have different half-lives.

The procedure is as follows. In a given run we measure the ratio of $\bar{n}(I)$ values at 8.8 A and some lower current. In these runs, a single source is prepared and moved into the counting position. With the proton beam turned off and the spectrometer current set at 8.8 A, we observe decay positrons for a period of typically 200 s. We then change the current to some value in the range 2–8 A and count for typically 1000 s. Because the counting rates are much higher for the excited-state transition than for the ground state, a few runs of this kind are sufficient to give good statistical accuracy.

To analyze the measurements for a given run, we first separate the data into segments in which the spectrometer current was fixed at one value or the other. For each segment we

[1]We use $n(p)$ for the total spectrum intensity, while $n_0(p)$ and $n_1(p)$ represent the contributions from the ground and first excited state, respectively.

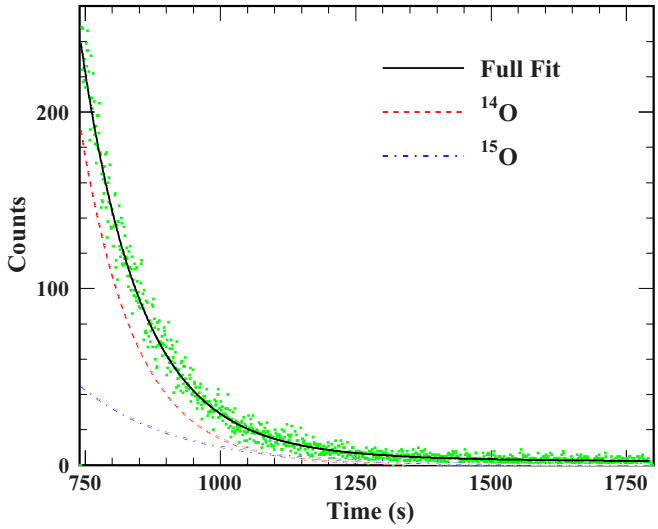


FIG. 3. (Color online) Sample decay curve for extracting the excited-state spectrum by lifetime decomposition. Data shown are for a spectrometer current corresponding to a momentum of 1.985 MeV/c. The points show the measured number of counts per 1-s interval, while the solid line is the fit obtained with the $A_i$'s of Eq. (7) treated as free parameters. The dashed and dot-dashed curves show the fit contributions from $^{14}$O and $^{15}$O. The $^{11}$C contribution ranges from 4 to 2 counts/s.

produce a Si(Li) energy spectrum. We then choose a window around the peak in the Si(Li) spectrum, and generate a decay curve, which gives counts within the window as a function of time in 1-s intervals.

For the measurements at the lower current, we fit the decay curve data with a three-term expression,

$$N(t) = A_1 e^{-t/\tau_1} + A_2 e^{-t/\tau_2} + A_3 e^{-t/\tau_3}, \tag{7}$$

where $\tau_1$, $\tau_2$, and $\tau_3$ are the mean lifetimes for $^{14}$O, $^{15}$O, and $^{11}$C, respectively, and where the $A$'s are the fitting parameters. Because the counting time is long compared to the mean lifetimes of both $^{14}$O and $^{15}$O, the average Si(Li) rate at the end of the counting interval is often less than 1/s. Consequently, we use Poisson statistics to optimize the fit to the decay curve measurements. A sample experimental decay curve and corresponding fit using Eq. (7) is shown in Fig. 3.

For the measurements at 8.8 A the acceptance of the spectrometer is at or above the $^{15}$O and $^{11}$C endpoints. Therefore, the decay curve was fit with a formula that includes an exponential term for $^{14}$O plus a constant to represent possible backgrounds. In the initial fits the background term was found to be statistically consistent with zero, and was subsequently fixed at zero for the final fits.

After obtaining the ratio of the $t = 0$ $^{14}$O rates at the two currents, we apply corrections for bad events, for backgrounds from 2.3 MeV $\gamma$ rays, and for good positron events that lie outside the Si(Li) summation window. Finally we convert the resulting $\bar{n}$ ratio to a ratio of $n(p)$ values.

The results are shown in Fig. 4. The plotted data points are the $n(p)$ values from which the small ground-state contributions have been subtracted. As in Fig. 2, the results

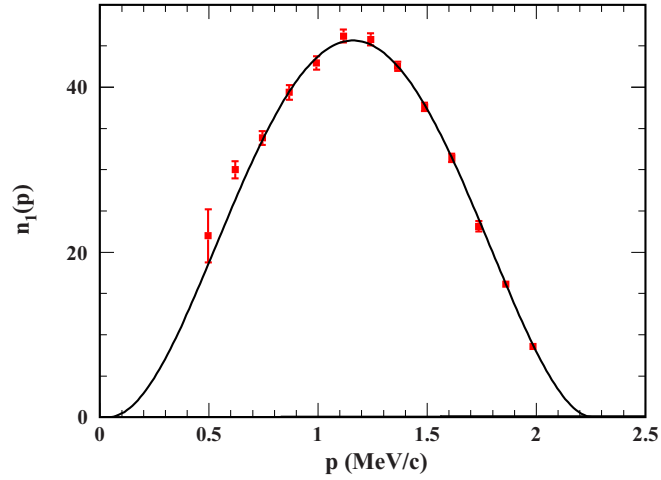


FIG. 4. (Color online) Measurements of the $^{14}$O $\beta$-spectrum intensity across the region dominated by the transition to first excited state of $^{14}$N. The measured points were extracted from decay curves, and are plotted on a scale set by the condition $n(p) = 1$ at a current of 8.8 A.

are normalized by the condition $n(p) = 1$ at 8.8 A, and the curve is once again a theoretical spectrum of the form given in Eq. (4), except that the shape factor $C(E)$ is now a constant.

For reasons to be explained later, we only use the measurements for momenta above $p = 0.9$ MeV/c in the determination of the branching ratio. Thus, the four lowest-momentum points in Fig. 4 are not employed. All of the data points shown are well above the endpoint of the transition to the second excited state of $^{14}$N.

## III. BRANCHING RATIO

The full decay rate $\lambda_i$ for either transition is obtained by integrating the corresponding $\beta$ spectrum:

$$\lambda_i^\beta = \int n_i(p)\, dp. \tag{8}$$

From the best fit curves shown in Figs. 2 and 4 we obtain the ratio of the positron decay rates for the ground-state ($\lambda_0^\beta$) and first excited-state ($\lambda_1^\beta$) transitions,

$$\frac{\lambda_0^\beta}{\lambda_1^\beta} = (4.965 \pm 0.040) \times 10^{-3}, \tag{9}$$

where the quoted uncertainty includes statistical errors only. Taking into account decays to the second excited state of $^{14}$N, for which the average measured branching ratio is $(0.545 \pm 0.019) \times 10^{-3}$ [1], and the relatively small rates for electron capture into the ground and first excited state [14], we obtain a ground-state branching ratio,

$$R = \frac{\lambda_0}{\lambda_{\text{total}}} = (4.934 \pm 0.040) \times 10^{-3}, \tag{10}$$

where $\lambda_0$ and $\lambda_{\text{total}}$ include contributions from both positron decay and electron capture.

### A. Systematic errors

In Fig. 2 we show the measured ground-state $\beta$ spectrum. These measurements cover only about half of the full momentum range, so extraction of the transition strength requires knowledge of the spectrum shape. Our assumed $\beta$ spectrum uses a shape factor parametrized in terms of the constants $a'$, $b'$, and $c'$ of Eq. (6).

From GVSK,

$$\begin{aligned} a' &= -0.0290 \pm 0.0008(\text{stat.}) \pm 0.0006(\text{syst.}), \\ b' &= \quad 0.04\ (\text{fixed}), \\ c' &= \quad 0.0061 \pm 0.0010(\text{stat.}) \pm 0.0005(\text{syst.}). \end{aligned} \tag{11}$$

As explained in GVSK, the quantity $W_c$ in Eq. (6) was chosen so that the statistical uncertainties in $a'$ and $c'$ are uncorrelated. For the present analysis we take the uncertainties in $a'$ and $c'$ to be the linear sums of the statistical and systematic errors listed in Eq. (11), and $\delta b' = 0.02$. The resulting systematic uncertainties in $R$ are $\pm\,\mathbf{0.009} \times \mathbf{10^{-3}}$ from $a'$, $\pm\mathbf{0.006} \times \mathbf{10^{-3}}$ from $b'$, and $\pm\mathbf{0.038} \times \mathbf{10^{-3}}$ from $c'$.

In our experiment, the Si(Li) energy spectra (see Fig. 1) have large background rates below typically channel 120. To determine the true event rate we sum the measured spectrum over some range of channels (typically 146–240 at 8.8 A and 150–290 at 11.0 A) and then apply a correction for subthreshold events. The procedure, which involves the use of experimental $^{66}$Ga spectra and Monte Carlo simulations, is described in GVSK. The uncertainty in the 11-A subthreshold correction leads to an uncertainty in the ground-state transition rate, and thus to a possible systematic error in the branching ratio. We estimate this systematic error to be $\pm\mathbf{0.012} \times \mathbf{10^{-3}}$.

In our analysis we notice that the extracted branching ratio changes by up to a few tenths of one percent as we move the 11-A lower summation threshold between channel 120 and channel 220 (see Fig. 1). This variation is larger than expected from uncertainties in the subthreshold correction, and to be on the safe side, we include an additional systematic uncertainty of $\pm\mathbf{0.019} \times \mathbf{10^{-3}}$ to cover this variation.

Subthreshold corrections are required for the excited-state measurements as well as for the ground state. High-quality $^{66}$Ga reference spectra are not available at these lower currents, although some clean $^{14}$O spectra (obtained under different circumstances) exist for currents between 4 and 8 A. At these low currents, the subthreshold counts arise from events in which the positron backscatters out of the Si(Li) detector without depositing its full energy. Our experience is that our Monte Carlo simulations tend to overpredict the number of such events [8], and comparisons of the simulations to the clean spectra show an excess of about 7% throughout the 4–8 A current range. With that information in hand we calculate the subthreshold corrections using simulations that have been scaled down by 7% in the backscattering region. To estimate the possible systematic error associated with the correction, we take the scale factor to be $1.07 \pm 0.07$. The resulting systematic error in the branching ratio is $\pm\mathbf{0.032} \times \mathbf{10^{-3}}$.

Systematic errors in the 8.8-A subthreshold correction cancel in the determination of the branching ratio, because we use the same summation windows and correction factors in the ground-state and excited-state analyses.

Contributions to the measured counting sums from background processes are small but not negligible. The various background effects are discussed in some detail in GVSK. The largest effect in the present experiment is the presence of counts within the 11-A summation window from 2.3-MeV $\gamma$ rays. We use Monte Carlo simulations to estimate the number of such events, and these simulations are subject to possible systematic errors. We estimate the resulting uncertainty in the branching ratio to be $\pm\mathbf{0.012} \times \mathbf{10^{-3}}$.

For the excited-state transition, there are significant contributions to the measured counting rates from events in which the positron backscatters from the aluminum backing foil. These and other "bad events" are estimated by Monte Carlo simulations and need to be subtracted. The required corrections are large at low momenta. For example, for the two lowest currents shown in Fig. 4, the bad event fractions are 17% and 9%. As noted earlier, we ignore the four lowest points in the determination of the branching ratio, and the result is that the bad event fractions are less than 2% for the points retained. The resulting systematic uncertainty in $R$ is $\pm\mathbf{0.006} \times \mathbf{10^{-3}}$.

To a good approximation, the spectrometer fields depend only on the magnet current. However, there are remnant fields from flux pinning in the superconducting magnets, and these fields depend on the current history. For the most part, the corrections are negligible except at 8.8 A where the slope of $n(p)$ is large. For the excited-state measurement we always approach 8.8 A from below, but the same is not true for the ground-state measurements. We use a model [9] to estimate the pinning correction and take the systematic uncertainty in $R$ to be $\pm\mathbf{0.020} \times \mathbf{10^{-3}}$.

The net systematic error is obtained by summing the contributions listed above in quadrature. The result is

$$\delta R = \pm 0.061 \times 10^{-3}. \tag{12}$$

A number of additional error sources were considered and found to be insignificant. These include uncertainties in the ground- and excited-state $Q$ values, uncertainties in the $^{14}$O and $^{15}$O half-lives, possible drifts in the spectrometer current, the spectrometer calibration uncertainty, and possible contributions to the 8.8-A counting rate from $^{15}$O decay.

### B. Comparison to previous measurements

As we noted in Sec. I, three previous measurements of the branching ratio have been reported.

Sidhu and Gerhart (SG) [5] obtained the value $R = (6.1 \pm 0.1) \times 10^{-3}$. A reanalysis of the SG measurements that includes the effects of the various correction factors appearing in Eq. (5) was carried out by Towner and Hardy [6]. They use $\beta$-decay shape factors derived from theoretical calculations that have been optimized to fit the SG data, and obtain $R = (5.4 \pm 0.2) \times 10^{-3}$.

We have also reanalyzed the SG data, and agree that the analysis employed by SG results in a branching ratio that is too high. We use the spectrum shape reported in GVSK and obtain $R = 5.5 \times 10^{-3}$. As seen previously in Ref. [6], the fit

to the SG data is not very good. In our reanalysis the total $\chi^2$ is 76 for 11 data points.

Additionally, we believe that SG have failed to account for a nontrivial systematic uncertainty. They determine the efficiency of their spectrometer by measuring the intensity of the excited-state transition at a kinetic energy of 1.691 MeV. At this point $n(p)$ has a somewhat large slope. SG claim that their spectrometer calibration (momentum vs current) is known to an accuracy of 1 part in $10^3$, and one finds that a 0.1% change in $p$ translates into a change in $n(p)$ of more than 3% at the calibration energy. Consequently, this effect, by itself, leads to an uncertainty of $\pm 0.2 \times 10^{-3}$ in $R$.

Taking into account the original $\pm 0.1 \times 10^{-3}$ error quoted by SG, the calibration uncertainty noted above, and uncertainties associated with the shape of the ground-state $\beta$ spectrum, we would quote $R = (5.5 \pm 0.3) \times 10^{-3}$ for our reanalysis of the SG data.

Earlier determinations of the branching ratio were reported by Sherr *et al.* [3] and by Frick *et al.* [4]. In both cases the authors determine $R$ from Kurie plots which were analyzed in the allowed approximation, i.e., with a Fermi function $F(p,Z) = F_0(p,Z)$ [see Eq. (5)] and with a constant $C(E)$ shape factor. As pointed out by Towner and Hardy [6], the allowed approximation is not adequate for the ground-state transition.

After describing their reanalysis of the measurements of Refs. [4,5], Towner and Hardy state "The conclusion is clear. For the Gamow-Teller branching ratio in $^{14}$O, determinations based on an allowed approximation analysis of Kurie plots have to be increased by about 14%." We do not agree with that conclusion.

Towner and Hardy draw their conclusion from analyses in which they determine the branching ratio by computing

$$R = \frac{f_{\rm GT}}{f_{\rm F}} \frac{X_{\rm GT}^2}{X_{\rm F}^2}, \tag{13}$$

where

$$X = \frac{1}{n_i} \sum_{i=1}^{n_i} X_i, \tag{14}$$

and

$$X_i = \frac{K(W_i)}{W_0 - W_i}, \tag{15}$$

and where $K(W_i)$ is either a data point from the Kurie plot for analysis in the allowed approximation, or a Kurie point modified by a shape correction factor for more accurate analyses. In Eqs. (14) and (15), each point in the Kurie plot is given equal weight in the determination of the transition strength $X$, independent of the uncertainties in the $K(W_i)$ values and the subsequent $X_i$'s.

We extract branching ratios from the published data sets first in the allowed approximation and then with the correction factors of Eqs. (5) and (6) (with the GVSK shape parameters) included. The resulting branching ratios increase by 8.4% for the data set of Ref. [4], 11% for the data set of Ref. [5], and 6.3% for our own data set, when the shape corrections are included.

Our reanalysis of the Ref. [4] data begins with the Kurie plots which the authors show in Fig. 7. Error bars are shown for three of the points plotted for the ground-state transition, and we take these to be representative of the entire data set. From the plotted $K(W_i)$ values we extract results for $n(p)$ (along with uncertainties), and fit the resulting data with the assumed $\beta$ spectrum by minimizing $\chi^2$. A similar procedure is used for the excited-state transition. For the excited state the distribution of errors is unimportant because the traditional allowed $\beta$ spectrum and the modified spectrum of Eq. (5) are very similar. Our reanalysis gives $\lambda_0/\lambda_1 = 6.46 \times 10^{-3}$ in the allowed approximation, in agreement with the result published in Ref. [4]. When the shape corrections are included, we obtain $\lambda_0/\lambda_1 = 7.0 \times 10^{-3}$.

Following analogous procedures we have also reanalyzed the data of Sherr *et al.* [3]. Here only the ground-state Kurie plot is shown, and no visible error bars are displayed. However, sample spectra are shown, which we integrate, using the sums to make error estimates. (For this data set the measurements are confined to a relatively narrow momentum range and consequently the deduced branching ratio is relatively insensitive to the assumed distribution of uncertainties.) After extracting the $n(p)$ values we fit the data set with allowed and GVSK $\beta$ spectra, and find that the GVSK spectrum gives a transition strength which is 10% larger than that of the allowed spectrum. No plot is shown for the excited-state transition, so we cannot extract a spectrum integral for this transition. However, we know that the shifts in the extracted branching ratios come almost entirely from the modification of the ground-state $\beta$ spectrum. Therefore, our analysis, crude as it may be, suggests inflating the branching ratio reported in Ref. [3] from $6.0 \times 10^{-3}$ to $6.6 \times 10^{-3}$.

In summary, we quote $R = (5.5 \pm 0.3) \times 10^{-3}$ from Ref. [5], $(6.6 \pm 1.0) \times 10^{-3}$ from Ref. [3], $(7.0 \pm 0.5) \times 10^{-3}$ from Ref. [4], and $(4.934 \pm 0.040 \pm 0.061) \times 10^{-3}$ from the present work.

## IV. DETERMINATION OF THE $\mathcal{F}t$ VALUE

We now wish to see what effect the new measurement has on the determination of the $^{14}$O $\mathcal{F}t$ value. We will follow the procedures adopted by Hardy and Towner [1]. First we take the error weighted average of the four branching ratio measurements listed above, taking the net error in the present measurement as the sum in quadrature of the systematic and statistical errors. The result is $R = (5.013 \pm 0.070) \times 10^{-3}$.

The set of measurements deviate from the mean with a reduced $\chi^2$ of 7.4. In view of this, the uncertainty needs to be scaled up by a factor $S$, which is taken to be the square root of the reduced $\chi^2$ recomputed using only those measurements with errors less than $3\sqrt{N}$ times the uncertainty in the average. In the present case, this condition eliminates Refs. [3] and [4] from the computation of the scale factor. We then obtain $S = 1.95$ giving

$$R = (5.013 \pm 0.137) \times 10^{-3}. \tag{16}$$

This is to be compared with the value $R = (5.71 \pm 0.68) \times 10^{-3}$ used previously in Ref. [1]. With the new branching

ratio, the uncertainty in the partial half-life for the $0^+$ decay is reduced from 50 to 15 ms.

In addition to the partial half-life, the value of $\mathcal{F}t$ also depends sensitively on the $Q$ value of the decay. The recent new measurement of this quantity [7] has reduced the uncertainty in $Q$ by nearly an order of magnitude. When combined with previous measurements of $Q$ (see Ref. [1]), one obtains a weighted mean of $Q_{EC} = 2831.564(0.027)$ keV. The corresponding value of the statistical weight factor $f$ is 42.8053(0.0027). This result was provided to us by Towner [15], and was computed with codes that use exact solutions of the Dirac equation. The recent Towner-Hardy [16] parametrization of the statistical weight factors gives the same result to the number of decimal places quoted.

Incorporating the updated value of $f$ along with the improved determination of the partial half-life, we obtain a corrected $\mathcal{F}t$ value of 3071.6(1.9) s. This is to be compared with 3071.4(3.2) s listed in Ref. [1], and 3073.8(2.8) s from Ref. [7], where the new $Q$-value measurement was incorporated for the first time. Our new result is in good agreement with the average superallowed $0^+ \rightarrow 0^+$ $\mathcal{F}t$ of 3072.27(0.62) s reported in Ref. [1].

## V. CONCLUSIONS

We have presented a new measurement of the $^{14}$O branching ratio which is significantly more accurate than any previous determination. With the new result included, the uncertainty in the weighted average of all measurements of this quantity is reduced by a factor of five. Correspondingly, the uncertainty in the partial half-life for the superallowed $0^+ \rightarrow 0^+$ Fermi decay to the $^{14}$N first excited state is reduced from 50 to 15 ms. Our new measurement combined with the recent accurate determination of the $Q$ value lead to an $\mathcal{F}t$ value whose uncertainty is reduced from 3.2 to 1.9 s. At the present time, this uncertainty is completely dominated by correction factors that depend on the nuclear structure of the $A = 14$ $0^+$ states.

Our result for the $^{14}$O corrected $\mathcal{F}t$ value is in good agreement with the average superallowed $0^+ \rightarrow 0^+$ $\mathcal{F}t$ reported in Ref. [1]. With the new $Q$-value measurement from Ref. [7] and our new determination of the branching ratio, $^{14}$O has the third lowest $\mathcal{F}t$ uncertainty of the "traditional 14" transitions which are used in the determination of the CKM $V_{ud}$ matrix element.

## ACKNOWLEDGMENTS

The authors wish to thank Ian Towner and John Hardy for many helpful comments during the course of the data analysis. We also thank Matthew Kowalski for his assistance on the project, and the University of Wisconsin Center for High Throughput Computing for allowing access to their computational facilities. This work was supported in part by the National Science Foundation under Grants No. PHY-0855514 and No. PHY-0555649, and in part by an allocation of time from the Ohio Supercomputer Center.

[1] J. C. Hardy and I. S. Towner, Phys. Rev. C **91**, 025501 (2015).
[2] A. T. Laffoley *et al.*, Phys. Rev. C **88**, 015501 (2013).
[3] R. Sherr, J. B. Gerhart, H. Horie, and W. F. Hornyak, Phys. Rev. **100**, 945 (1955).
[4] G. Frick, A. Gallmann, D. E. Alburger, D. H. Wilkinson, and J. P. Coffin, Phys. Rev. **132**, 2169 (1963).
[5] G. S. Sidhu and J. B. Gerhart, Phys. Rev. **148**, 1024 (1966).
[6] I. S. Towner and J. C. Hardy, Phys. Rev. C **72**, 055501 (2005).
[7] A. A. Valverde, G. Bollen, M. Brodeur, R. A. Bryce, K. Cooper, M. Eibach, K. Gulyuz, C. Izzo, D. J. Morrissey, M. Redshaw, R. Ringle, R. Sandler, S. Schwarz, C. S. Sumithrarachchi, and A. C. C. Villari, Phys. Rev. Lett. **114**, 232502 (2015).
[8] E. A. George, P. A. Voytas, G. W. Severin, and L. D. Knutson, Phys. Rev. C **90**, 065501 (2014).
[9] L. D. Knutson, G. W. Severin, S. L. Cotter, L. Zhan, P. A. Voytas, and E. A. George, Rev. Sci. Instrum. **82**, 073302 (2011).
[10] D. E. Alburger, Rev. Sci. Instrum. **27**, 991 (1956).
[11] D. H. Wilkinson, Nucl. Instrum. Meth. A **290**, 509 (1990).
[12] A. Sirlin, Phys. Rev. **164**, 1767 (1967).
[13] D. H. Wilkinson, Nucl. Instrum. Meth. A **335**, 182 (1993).
[14] W. Bambynek, H. Behrens, M. H. Chen, B. Crasemann, M. L. Fitzpatrick, K. D. Ledingham, H. Genz, M. Mutterer, and R. L. Intemann, Rev. Mod. Phys. **49**, 77 (1977).
[15] I. S. Towner (private communication).
[16] I. S. Towner and J. C. Hardy, Phys. Rev. C **91**, 015501 (2015).